

IL NUOVO CIMENTO  
DOI 10.1393/ncc/i2012-11113-1

VOL. 35 C, N. 1

Gennaio-Febbraio 2012

COLLOQUIA: LaThuile11

## Electroweak physics at the Tevatron

J. SEKARIC for the CDF and DØ COLLABORATIONS

*Department of Physics and Astronomy, University of Kansas - Lawrence, KS 66045, USA*

(ricevuto il 29 Settembre 2011; pubblicato online il 17 Gennaio 2012)

**Summary.** — The most recent Electroweak results from the Tevatron are presented. The importance of precise Standard Model measurements in the Higgs sector, quantum chromodynamics and searches for new physics is emphasized. Analyzed data correspond to  $1\text{--}7\text{ fb}^{-1}$  of integrated luminosity recorded by the CDF and DØ detectors at the Tevatron Collider at  $\sqrt{s} = 1.96\text{ TeV}$  during the period between 2002 and 2010.

PACS 12.15.Ji – Applications of electroweak models to specific processes.

PACS 13.85.Qk – Inclusive production with identified leptons, photons, or other nonhadronic particles.

PACS 14.70.Fm –  $W$  bosons.

PACS 14.70.Hp –  $Z$  bosons.

### 1. – Introduction

The main goal of the Electroweak (EW) physics is to probe the mechanism of the EW symmetry breaking. An important aspect of these studies is related to precise measurements of the Standard Model (SM) parameters and tests of the  $SU(2) \times U(1)$  gauge symmetry. Deviations from the SM may be indicative of new physics. Thus, the interplay between the tests of the “standard” physics and searches for a “non-standard” physics is an important aspect of the EW measurements. The observables commonly used in these measurements are cross sections, gauge boson couplings, differential distributions, asymmetries, etc. Besides, many EW processes represent a non-negligible background in a Higgs boson and top quark production, and production of supersymmetric particles. Therefore, the complete and detailed understanding of EW processes is a mandatory precondition for early discoveries of very small new physics signals. Furthermore, several EW analyses represent a proving ground for analysis techniques and statistical treatments used in the Tevatron Higgs searches.

### 2. – Single-boson production

Measurements of gauge boson properties such as mass, differential distributions and production asymmetries represent an important input to theoretical predictions which will provide a better description of Tevatron data and increase sensitivity to new physics signals.

Precise measurements of the  $W$  boson mass are important, because they restrict the phase space of the so far unseen SM Higgs and set indirect constraints on new physics via EW radiative corrections. At the Tevatron, the  $W$  boson mass is measured using three kinematic variables: lepton transverse momentum,  $p_T^l$  (where  $l = e, \mu$ ), imbalance in transverse energy arising from the neutrino,  $p_T^\nu$  (often referred as to missing  $E_T$ ), and the  $W$  boson transverse mass defined as  $M_T = \sqrt{2p_T^l p_T^\nu (1 - \cos \Delta\phi)}$ , where  $\Delta\phi$  is the opening angle between the electron (muon) and neutrino momenta in the plane transverse to the beam. Correct modeling of the hadronic recoil from the QCD radiation is highly important for  $W$  mass measurement as it balances the boson's  $p_T$ . CDF selects events with  $p_T^l > 18$  (30) GeV/ $c$  in the electron (muon) channel, missing  $E_T > 30$  GeV and  $|\vec{u}| < 15$  GeV/ $c$  in  $0.2 \text{ fb}^{-1}$  of integrated luminosity using both the electron and muon channel. DØ selects events with  $p_T^l > 25$  GeV/ $c$ , missing  $E_T > 25$  GeV and  $|\vec{u}| < 15$  GeV/ $c$  in  $1.0 \text{ fb}^{-1}$  of integrated luminosity using only the electron channel. Both experiments use all three reconstructed variables to measure the  $W$  boson mass. CDF measures  $q$   $W$  mass of  $80.413 \pm 0.034$  (stat)  $\pm 0.034$  (syst) GeV/ $c^2$  [1]. DØ measures the  $W$  mass to be  $80.401 \pm 0.021$  (stat)  $\pm 0.038$  (syst) GeV/ $c^2$  [2] which represents the most precise single  $W$  mass measurement to date. Using the same data DØ extracts the width of the  $W$  boson to be  $\Gamma_W = 2.028 \pm 0.039$  (stat)  $\pm 0.061$  (syst) GeV using  $M_T$  distribution [3].

The production of single  $W$  bosons in  $p\bar{p}$  collisions also provides information on the momentum fraction dependence of the  $u$  and  $d$  quark parton distribution functions (PDF) within the proton. The boost along the  $z$ -axis in the direction of more energetic parton causes an asymmetry in the  $W$  boson and charged lepton production. After data has been corrected for detector effects, efficiencies, charge mis-identification, etc, the asymmetry  $A$  is measured as a function of rapidity  $y_W$  of the  $W$  boson or pseudorapidity  $\eta_l$  of charged lepton, and transverse momentum. Current results on lepton charge asymmetry from  $1 \text{ fb}^{-1}$  of CDF integrated luminosity, electron charge asymmetry from  $0.75 \text{ fb}^{-1}$  of DØ integrated luminosity [4] and muon charge asymmetry from  $5 \text{ fb}^{-1}$  of DØ integrated luminosity [5], show mutual disagreement when split in different lepton  $p_T$  bins. In addition, both CDF and DØ lepton charge asymmetries do not agree with CTEQ6.6 PDF prediction when split into  $p_T$  bins while  $W$  boson asymmetry measured by CDF agrees well with higher-order predictions [6].

The study of  $Z$  boson kinematic distributions is yet another test that contributes to the tuning of theoretical QCD predictions. Distributions such as transverse momentum, rapidity and  $\phi_\eta^*$  of dilepton pairs are studied at the Tevatron.

The differential cross section as a function of the dimuon  $p_T$  distribution has been studied with  $1 \text{ fb}^{-1}$  of integrated luminosity recorded at DØ. Unfolded data normalized to the PYTHIA Perugia 6 prediction is compared to other generators as shown in fig. 1. In the low  $p_T$  region ( $Z$   $p_T < 30$  GeV) the resummation describes data well while the high  $Z$   $p_T > 30$  GeV region shows the best shape agreement with higher-order perturbative QCD but with an offset in normalization. Since the  $p_T$  distribution is sensitive to resolution effects, the  $\phi_\eta^*$  distribution based exclusively on angular resolution is an excellent place to probe QCD predictions with higher precision. It is defined as  $\phi_\eta^* = \tan(\phi_{acop}/2) \sin(\theta)_\eta^*$  where  $\phi_{acop}$  is the acoplanarity angle  $\phi_{acop} = \pi - \Delta\phi_{ll}$  and  $\Delta\phi_{ll}$  is the difference in azimuthal angle  $\phi$  between the two leptons. The variable  $(\theta)_\eta^*$  is defined as  $(\theta)_\eta^* = a \cos[\tanh(\eta^- - \eta^+)/2]$  where  $\eta^-$  and  $\eta^+$  are the pseudorapidities of the negatively and positively charged lepton, respectively. As presented in fig. 2 where the ratio of the corrected distribution  $(1/\sigma) \times (d\sigma/d\phi_\eta^*)$  to RESBOS is shown for three different rapidity

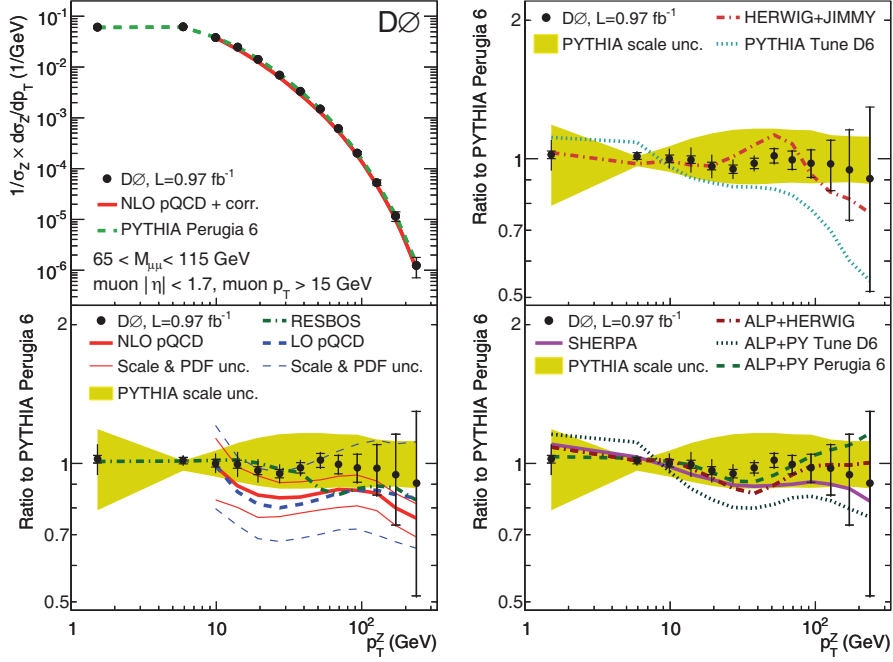


Fig. 1. – The normalized differential cross section and its ratio relative to PYTHIA Perugia 6 in bins of  $Z p_t$  for  $Z/\gamma^*(\rightarrow \mu\mu) + X$  events. The data are shown with statistical and systematic uncertainties. The distribution is compared to different generators and NLO predictions.

regions, predictions from RESBOS fail to describe the detailed shape of the data, and a prediction that includes the effect of small- $x$  broadening is disfavored.

The CDF experiment performs a measurement of  $d\sigma/dy$  selecting  $Z/\gamma^* \rightarrow e^+e^-$  events in the mass range of 66 to 116  $\text{GeV}/c^2$  using data of  $2.1 \text{ fb}^{-1}$  of integrated luminosity. The comparison of unfolded data to different QCD predictions shows a good agreement as presented in fig. 3. The measured cross section for  $Z$  production of  $\sigma_Z \times BR(Z \rightarrow e^+e^-) = 256.6 \pm 15.5$  (stat + syst) pb is in good agreement with higher order QCD predictions. In addition, the selected data is used to extract  $p_T$  dependent angular coefficients,  $A_0, A_2, A_3$  and  $A_4$ . The  $p_T$  dependence of  $A_0$  and  $A_2$  is found to be in agreement with the predictions of perturbative QCD, confirming the Lam-Tung relation which implies that the spin of the gluon is 1 if  $A_0 = A_2$ . The values of  $A_3$  and  $A_4$  are in agreement with the predictions of all QCD models [7]. The measured  $A_4$  is used to extract  $\sin^2 \theta_W = 0.2329 \pm 0.0008_{-0.0009}^{+0.0010}$  (QCD) as shown in fig. 3.

### 3. – Diboson production

As an important production mechanism for understanding the EW symmetry breaking, diboson physics focuses on precise measurements of the cross section and the trilinear gauge boson couplings (TGCs) [8]. Besides, the most precise knowledge of these processes and their proper modeling is highly valuable in many searches for new physics which may exist at some energy scale  $\Lambda$ . The quantity  $\Lambda$  is physically interpreted as the mass scale where the new phenomenon responsible for the anomalous couplings is directly observable.

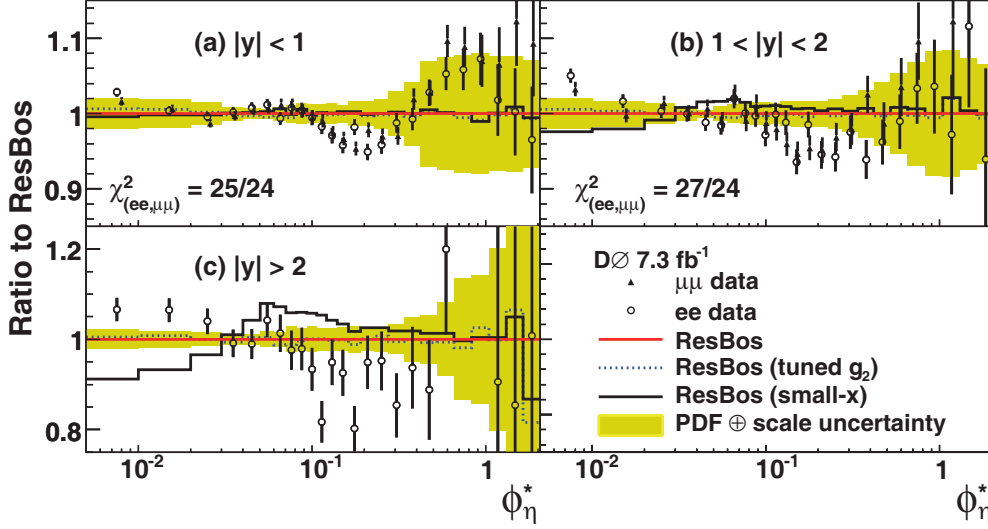


Fig. 2. – Ratio of  $(1/\sigma) \times (d\sigma/d\phi_\eta^*)$  to RESBOS in different  $Z$  rapidity bins. The yellow band around the RESBOS prediction represents the quadrature sum of uncertainty due to CTEQ6.6 PDFs and the uncertainty due to the QCD scale. Comparisons to the RESBOS predictions when  $g_2$  is set to  $0.66 \text{ GeV}^2$  (dotted blue line) and to the small- $x$  broadening (solid black line) are shown as well.

The  $Z\gamma \rightarrow l^+l^-\gamma$  ( $l = e, \mu$ ) and  $Z\gamma \rightarrow \nu\bar{\nu}\gamma$  events selected from the CDF data of  $5 \text{ fb}^{-1}$  of integrated luminosity have a photon with transverse energy  $E_T > 50 \text{ GeV}$  which is spatially separated from a lepton by  $\Delta R_{l\gamma} > 0.7$ . Charged leptons are required to have  $p_T > 20 \text{ GeV}/c$  ( $E_T > 20 \text{ GeV}$ ) for one muon (electron) candidate and  $p_T > 10 \text{ GeV}/c$  ( $E_T > 10 \text{ GeV}$ ) for the other. The three-body mass cut of  $100 \text{ GeV}$  is applied to separate

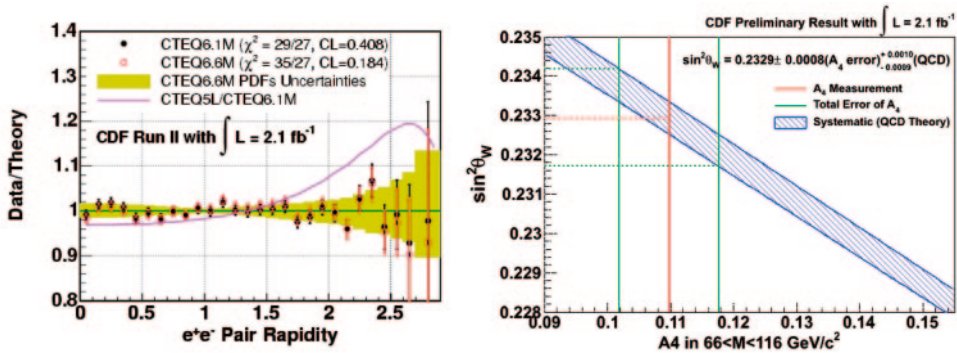


Fig. 3. – (Colour on-line) Left: Ratio of data to theory prediction for  $(1/\sigma) \times (d\sigma/dy)$ . The prediction uses PYTHIA MC with NLO CTEQ6.1M and CTEQ6.6M PDFs. Right: The value of  $\sin^2 \theta_W$  as a function of  $A_4$ . Measured values of  $\sin^2 \theta_W$  and  $A_4$  are shown in red, and the blue band corresponds to different QCD predictions. The green lines represent the total uncertainty from measurement of  $A_4$ .

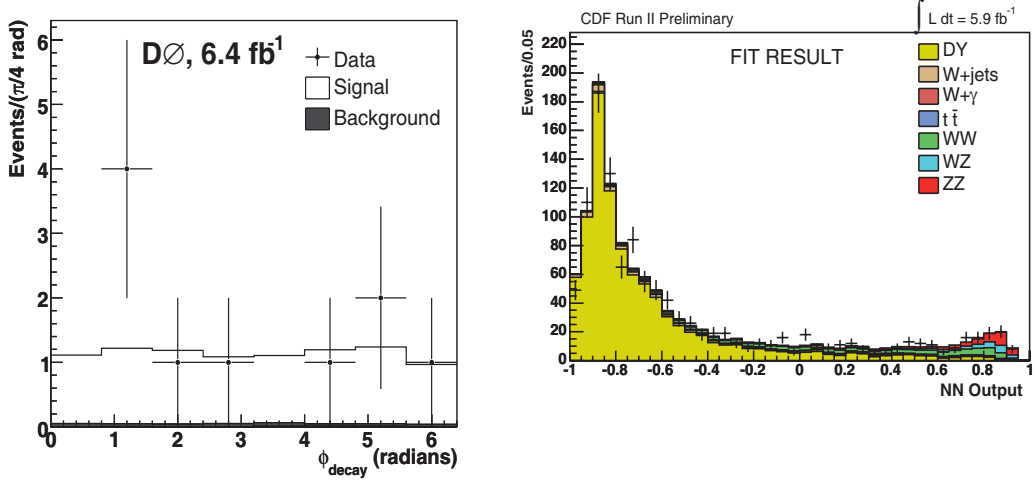


Fig. 4. – Left: The azimuthal angle decay distribution of the  $Z/\gamma^*$  candidates selected in the  $ZZ \rightarrow \bar{l}l'\bar{l}'$  analysis, compared to the expected signal and background. Right: The Neural Network output used in the fit to the data to measure the  $ZZ$  cross section.

events which originate from the final-state radiation. Photon  $E_T$  spectra from  $l^+l^-\gamma$  and  $\nu\bar{\nu}\gamma$  candidate events are combined and used to set the limits on  $Z\gamma\gamma/ZZ\gamma$  TGCs. The one-dimensional 95% CL limits on  $h_{3,4}^{\gamma,Z}$  at  $\Lambda = 1.5$  TeV are  $-0.017 < h_3^{Z,\gamma} < 0.016$ ,  $-0.0006 < h_4^Z < 0.0005$  and  $|h_4^\gamma| < 0.0006$ . They are the most restrictive limits on these couplings to date [9].

The  $\phi_{decay}$  distribution of ten  $ZZ \rightarrow \bar{l}l'\bar{l}'$  ( $l, l' = e, \mu$ ) candidate events observed in  $D\bar{O}$  data of  $6.4\text{fb}^{-1}$  of integrated luminosity with a significance of 6 standard deviations are shown in fig. 4. The  $\phi_{decay}$  distribution is sensitive to different

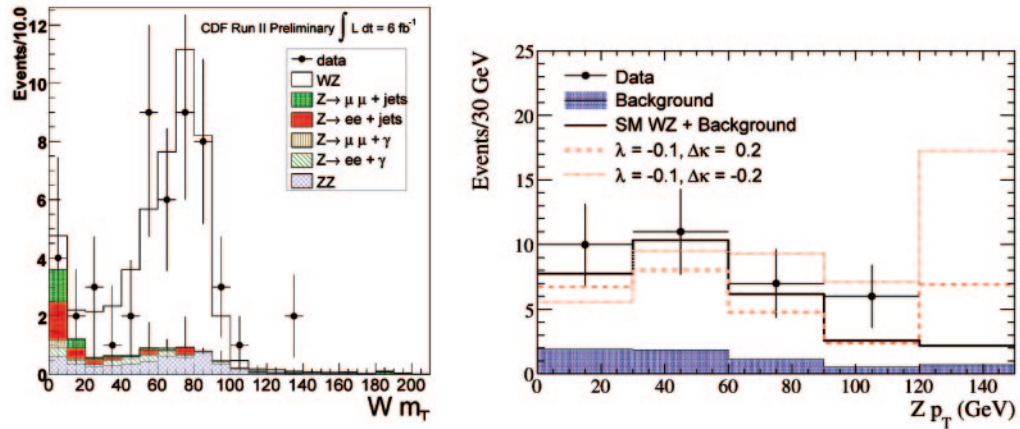


Fig. 5. – Left: Transverse mass of  $W$  bosons in  $WZ$  candidates. Right: Comparison of the  $Z$  boson  $p_T$  spectrum from data, total background, the SM  $WZ$  signal+total background and two TGC models.

scalar models arising from new physics [10]. The measured cross section is  $\sigma_{ZZ} = 1.24_{-0.37}^{+0.47}$  (stat)  $\pm 0.11$  (syst)  $\pm 0.08$  (lumi) pb and it represents the most precise  $\sigma_{ZZ}$  measurement at a hadron collider to date [11]. The  $ZZ \rightarrow l\bar{l}\nu\bar{\nu}$  ( $l = e, \mu$ ) events selected from data of  $5.9 \text{ fb}^{-1}$  of integrated luminosity at CDF were used to measure the cross section of  $\sigma_{ZZ} = 1.45_{-0.51}^{+0.60}$  (stat + syst) pb [12]. The Neural Network output shown in fig. 4 is used in analysis to separate  $ZZ$  events from the most dominant Drell-Yan background. The measured  $ZZ$  cross sections are in agreement with the SM prediction.

The most precise measurement of the  $WZ \rightarrow l\nu ll$  cross section has been recently performed by the CDF Collaboration. The analysis selects events with missing  $E_T > 25 \text{ GeV}$  and leptons of  $p_T > 15 \text{ GeV}/c$  where two leptons are of the same flavour, opposite charge and lie in the mass window  $(m_{ll} - M_Z) < 15 \text{ GeV}/c^2$ . After the final selection 50 candidate events are selected with expected background of  $11.2 \pm 1.63$  events. The  $WZ$  cross section, measured relative to the  $Z$  cross section is  $\sigma_{WZ}/\sigma_Z = [5.5 \pm 0.8 \text{ (stat)} \pm 0.5 \text{ (syst)}] \cdot 10^{-4}$ . Using a next-to-NLO calculation of the  $\sigma_Z \cdot \text{BR}(Z \rightarrow ll) = (251.3 \pm 5) \text{ pb}$  gives the cross section of  $\sigma_{WZ} = 4.1 \pm 0.6 \text{ (stat)} \pm 0.4 \text{ (syst)} \text{ pb}$  [13]. The DØ Collaboration measures the  $\sigma_{WZ}$  cross section selecting events in the same final states, requiring lepton candidates with  $p_T > 15 \text{ GeV}/c$  and missing  $E_T > 20 \text{ GeV}$ . The selection yields 34  $WZ$  candidate events with an estimated  $23.3 \pm 1.5$  signal, and  $6.0 \pm 0.6$  background events. The measured cross section of  $\sigma_{WZ} = 3.90_{-0.85}^{+1.01}$  (stat + syst)  $\pm 0.31$  (lumi) pb.

In addition,  $Z p_T$  spectrum shown in fig. 5 is used to set the limits on  $WWZ$  TGCs. The one-dimensional 95% CL limits on  $\Delta\kappa_Z, \lambda_Z$  and  $\Delta g_1^Z$  at  $\Lambda = 2.0 \text{ TeV}$  are  $-0.376 < \Delta\kappa_Z < 0.686$ ,  $-0.075 < \lambda_Z < 0.093$  and  $-0.053 < \Delta g_1^Z < 0.156$ . They are the best limits on these couplings to date as measured from direct  $WZ$  production [14].

#### 4. – Summary

The most recent EW results from CDF and DØ Collaborations using Tevatron data of  $1\text{--}7 \text{ fb}^{-1}$  of integrated luminosity have been presented. The  $W$  mass, cross sections and TGCs are measured with the best precision to date at a hadron collider. Observations are in agreement with the SM predictions though some discrepancies with theoretical predictions have been observed.

#### REFERENCES

- [1] AALTONEN T. *et al.* (CDF COLLABORATION), *Phys. Rev. Lett.*, **99** (2007) 151801.
- [2] ABAZOV V. *et al.* (D0 COLLABORATION), *Phys. Rev. Lett.*, **103** (2009) 141801.
- [3] ABAZOV V. *et al.* (D0 COLLABORATION), *Phys. Rev. Lett.*, **103** (2009) 231802.
- [4] ABAZOV V. *et al.* (D0 COLLABORATION), *Phys. Rev. Lett.*, **101** (2008) 211801.
- [5] ABAZOV V. *et al.* (D0 COLLABORATION), D0 Note 5976-CONF (2009).
- [6] AALTONEN T. *et al.* (CDF COLLABORATION), *Phys. Rev. Lett.*, **102** (2009) 181801.
- [7] AALTONEN T. *et al.* (CDF COLLABORATION), *Phys. Rev. Lett.*, **106** (2011) 241801, arXiv:1103.5699v3 [hep-ex] (2011).
- [8] HAGIWARA K., WOODSIDE J. and ZEPPENFELD D., *Phys. Rev. D*, **41** (1990) 2113.
- [9] AALTONEN T. *et al.* (CDF COLLABORATION), *Phys. Rev. Lett.*, **107** (2011) 051802, arXiv:1103.2990v1 [hep-ex] (2011).
- [10] CAO Q. *et al.*, *Phys. Rev. D*, **81** (2010) 015010.
- [11] ABAZOV V. *et al.* (D0 COLLABORATION), *Phys. Rev. D*, **84** (2011) 011103, arXiv:1104.3078v1 [hep-ex] (2011).
- [12] AALTONEN T. *et al.* (CDF COLLABORATION), CDF Note 10358 (2010).
- [13] AALTONEN T. *et al.* (CDF COLLABORATION), CDF Note 10238 (2010).
- [14] ABAZOV V. *et al.* (D0 COLLABORATION), *Phys. Lett. B*, **695** (2011) 67.